Investigation of deuterium trapping and release in the JET divertor during the third ILW campaign using TDS

J. Likonen[a,f,*], K. Heinola[b,f], A. De Backer[c,f], A. Baron-Wiechec[c,f], N. Catarino[d,f], I. Jepu[c,e,f], C.F. Ayres[c,f], P. Coad[c,f], G.F. Matthews[c,f], A. Widdowson[c,f], JET Contributors[1]

[a] VTT Technical Research Centre of Finland, P.O.Box 1000, FIN-02044 VTT, Finland
[b] University of Helsinki, P.O. Box 64, 00560 Helsinki, Finland
[c] CCFE, Culham Science Centre, Abingdon, Oxon, OX14 3DB, UK
[d] IPFN Instituto Superior Técnico, Universidade de Lisboa, 1049-001 Lisboa, Portugal
[e] National Institute for Laser, Plasma and Radiation Physics (NILPRP), Magurele 077125, Romania
[f] EUROfusion Consortium, JET, Culham Science Centre, Abingdon OX14 3DB, UK

A B S T R A C T

Selected set of samples from JET ITER-Like Wall (JET-ILW) divertor tiles exposed in 2015–2016 has been analysed using Thermal Desorption Spectrometry (TDS). The deuterium (D) amounts obtained with TDS were compared with Nuclear Reaction Analysis (NRA). The highest amount of D was found on the top part of inner divertor which has regions with the thickest deposited layers as for divertor tiles removed in 2014. This area resides deep in the scrape-off layer and plasma configurations for the second (ILW-2, 2013–2014) and the third (ILW-3, 2015–2016) JET-ILW campaigns were similar. Agreement between TDS and NRA is good on the apron of Tile 1 and on the upper vertical region whereas on the lower vertical region of Tile 1 the NRA results are clearly smaller than the TDS results. Inner divertor Tile 3 has somewhat less D than Tiles 0 and 1, and the D amount decreases towards the lower part of the tile. The D retention at the divertor inner and outer corner regions is not symmetric as there is more D retention poloidally at the inner than at the outer divertor corner. In most cases the TDS spectra for the ILW-3 samples are different from the corresponding ILW-2 spectra because HD and D_2 release occurs at higher temperatures than from the ILW-2 samples indicating that the low energy traps have been emptied during the plasma operations and that D is either in the energetically deep traps or located deeper in the sample.

1. Introduction

JET has now operated three operational periods with the ITER-like Wall – 2011–2012 (ILW-1), 2013–2014 (ILW-2) and 2015–2016 (ILW-3) so it offers a unique opportunity to study plasma-wall interactions (PWI) that will take place whilst operating the next step fusion device ITER. In the JET-ILW, the main chamber comprises of solid Be limiters, and the divertor consists of W-coated CFC tiles and load bearing tiles made of solid W. Gas balance measurements at JET performed during the ILW-1 have shown a factor of 10–20 reduction in the long term fuel retention resulting from the change of wall material from the all-carbon (JET-C) to the JET-ILW material combination [1,2]. Post-mortem analyses of the ILW-2 divertor tiles showed a reduction by a factor of >18 in the global fuel retention rate when compared to JET-C [1]. Moreover, the post-mortem analyses showed that the overall deposition pattern at the divertor had changed completely; during the JET-C the thickest deposits were at both shadowed regions of the divertor whereas in JET-ILW deposition occurred mainly on top of the inner divertor [3]. This indicated that the erosion and deposition processes had changed in

the JET-ILW and that the long range multistep migration process of eroded particles was missing due to lack of chemical sputtering [4].

The ILW-1 campaign concentrated on plasma scenarios most relevant for ITER, i.e. the strike points were on Tiles 3 and 5. The ILW-2 and ILW-3 campaigns, however, focussed on high power and high density plasma scenarios [5] with the inner strike points (ISP) on Tiles 3 and 4, and the outer strike points (OSP) on Tile 6. In addition, the ILW-2 operations ended in a two-week hydrogen campaign.

The present work continues the retention studies using the TDS technique by analysing JET divertor tiles installed during 2014–2015 shutdown and removed from the vessel after the ILW-3 experimental campaign. TDS results for ILW-3 samples will be compared with the D amounts measured with NRA and with TDS data obtained for ILW-2 tiles removed in 2014.

2. Experimental methods

The ILW-3 campaigns in 2015–2016 were run with 23.4 h of total plasma time of which 18.5 h were the divertor phase and 4.9 h the
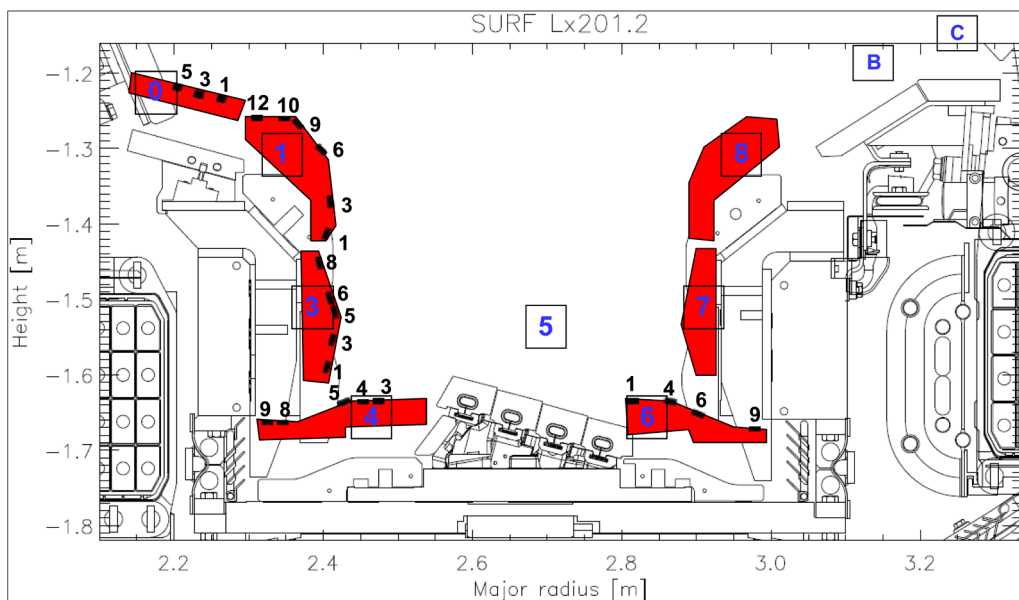

Fig. 1. Cross-section of the JET-ILW divertor. The divertor W-coated CFC tiles highlighted in red and the tile numbering from Tile 0 to Tile 8 is from the high field to the low field side, correspondingly. Small numbers show the location of analysed TDS samples. Samples are identified by tile number (Tile n) and then by location (m) and are referred to as e.g. 1/9, i.e. sample 9 from Tile 1. (For interpretation of the references to colour in this figure legend, the reader is referred to the web version of this article.)

limiter phase. The ILW-3 campaign consisted of a larger number of high power pulses with the total input energy (245 GJ) being somewhat higher than for the ILW-2 (201 GJ) in 2013–204.

Fig. 1 shows the poloidal cross section of the ILW divertor and highlights all the plasma-facing divertor tiles and samples that were analysed in this work. The plasma strike point distributions on the divertor tiles during the ILW-2 and ILW-3 campaigns are shown in Fig. 2. The strike point distributions for ILW-2 and ILW-3 are rather similar, the inner strike point (ISP) was mainly on Tile 3 and on the sloping part of Tile 4. During the ILW-2 and ILW-3 the outer strike point (OSP) was mainly on the sloping part of Tile 6 but there were discharges with the OSP on bulk W Tile 5.

The analysed JET-ILW W-coated CFC divertor tiles exposed during ILW-3 campaign in 2015–2016 consist either of 10–15 µm thick W coating (tiles HFGC 14N LH, 2BNG4C) or of 20–25 µm thick W coating (tiles 14IN G1C, 14BN G6D), all with ~3 µm thick Mo interlayer between the coating and the CFC substrate. Tile 2IW G3A has a marker coating with a layer structure of CFC (bulk)/Mo (3 µm)/W (12 µm)/Mo (4 µm)/W (4 µm). Outer divertor Tiles 7 and 8 will be analysed later. Comparison is made with tiles exposed during ILW-2 campaign.

Samples for the present studies were cut from each tile using a coring drill; the drill had an outside diameter of 20 mm and produced a core sample of 17 mm in diameter [6]. A poloidal line of holes was drilled every 20 mm across the tile. For the TDS analyses two topmost

discs with thicknesses of ~1 mm were cut from the cored samples from their plasma-facing sides. The resulted TDS amounts for D represent a D depth profile of 0–1 mm (disc with W-coating and bulk CFC) and 1.5–2.5 mm (only bulk CFC) the offset of 0.5 mm being due to the thickness of the saw blade. Samples are identified by tile number (Tile n) and then by location (m), and are referred to as e.g. 1/1, i.e. sample 1 from Tile 1 (see Fig. 1).

The TDS system at CCFE manufactured by Hiden Analytical Ltd (TPD Workstation type 640100) was used to anneal the cored divertor tile samples (see Fig. 1). The details of the TDS instrument with a base pressure typically of ~10^{-9} mbar have been reported extensively in a recent article [7]. The samples were annealed with a linear ramp rate (10 °C/min) from room temperature (RT) up to 1000 °C. A thermocouple is embedded in the Mo stage which has direct contact with the sample. The sample surface temperature and the heater temperature are also measured by an infrared pyrometer. The error in the temperature measurement is estimated to be ~20 °C. The released gases were measured with a line-of-sight quadrupole mass spectrometer as a function of time and annealing temperature. The TDS data was collected for mass-to-charge ratios corresponding to various molecules, e.g. H_2, HD, D_2, DT and T_2. The D signal was calibrated with an ion implanted D reference sample and the calibration procedure has been explained in detail in Ref. [7]. Polycrystalline W samples were implanted with a 30 keV D^+ beam to a dose of 5.8×10^{16} cm^{-2} at the University of Helsinki. The energy chosen is high enough for creating sufficient amounts of implantation-induced defects for trapping D in W at RT. Hydrogen has high diffusivity in W, so the retained D is in the implantation-induced defects (mainly vacancy-type defects), or in intrinsic defects, which can trap hydrogen at RT. During the implantation the remained D in solute sites can be considered to be diffused away from the bulk region of the sample once the implantation has finished. Detailed analysis on the 30 keV/D implantation-induced defect creation and the D retention has been provided in [8]. The absolute amount of the retained D in the implanted samples was determined experimentally with Time-of-flight Elastic Recoil Detection Analysis (TOF-ERDA) technique. The obtained result was 3.5×10^{16} D/cm^2, which is sufficient D amount for TDS. The calibration procedure used applies only for D and only rough estimations e.g. on T amounts can be made.

NRA measurements were made at IST (Lisbon) using ^{3}He ions at an energy of 2.3 MeV for determining the amounts of deuterium using the $D(^3He,p)^4$He reaction [9]. The size of beam was 1 mm in diameter. The 2.3 MeV ^{3}He beam allows to obtain the deuterium information up to a
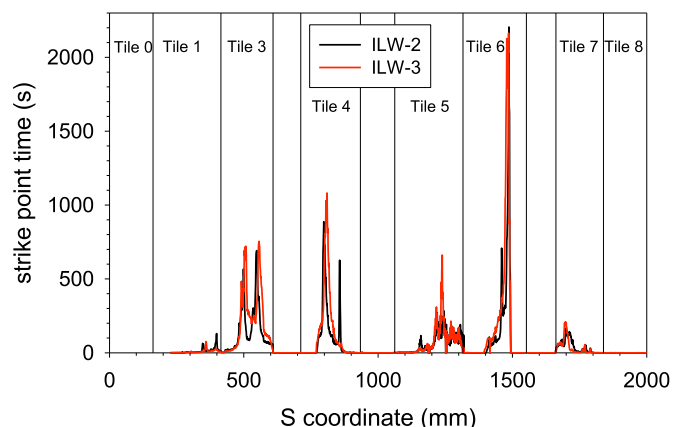

Fig. 2. Strike point distribution for ILW-2 (2013–2014) and ILW-3 (2015–2016).

depth of 9.0 μm in Be and 3.6 μm in W.

SIMS measurements were made using a double focusing magnetic sector instrument VG Ionex IX-70S at VTT. A 5 keV O_2^+ primary beam with a current of 500 nA was used [6]. D-implanted Be, Mo and W samples, which were analysed with Heavy Ion Elastic Recoil Detection Analysis (HI-ERDA) at University of Helsinki, were used for quantification of the SIMS measurements for deuterium. After the SIMS measurements, the depths of the craters were measured with a profilometer. The accuracy of the depth scales is estimated to be ± 20%.

3. Results and discussion

3.1. Inner divertor

The main material migration mechanism at JET during the ILW-3 campaign is still Be erosion at the main wall by hydrogen isotopes, other impurities and charge exchange neutrals, and transport during the X-point phase of the plasma towards the inner divertor. Tile 0 and the top horizontal part (apron) and the top plasma facing surface of Tile 1 were deep in the plasma scrape-off layer (SOL) during the ILW-3 and thick impurity layers were formed by the erosion of the main wall Be limiters. Moreover, D fuel was co-deposited in these layers.

Thicknesses of the co-deposited Be layers on the analysed samples is shown in Fig. 3. The thickest co-deposited layers are found on Tiles 0, and on apron and on top vertical part of Tile 1. The location and D amounts of the analysed samples are given in Table 1.

Fig. 4 shows TDS spectra for H_2, HD, D_2, and T_2 together with the sample temperature for the ILW-3 sample 0/1 exposed in 2015–2016 which has a thick Be co-deposited layer with a thickness of ~8 μm. The desorption spectra are fairly broad with at least four release maxima. Desorption of HD starts at ~90 °C whereas D_2 starts to be released at slightly higher temperature (~120 °C). T_2 release appeared to be very small. The total D amount (3.2×10^{18} atoms/cm^2) in sample 0/1 is obtained by integrating over the HD and D_2 signals and using the calibration factor determined with the ion implanted reference sample. The D_2 signal has broad release maxima at ~570 and at ~790 °C but both D_2 and HD signals have clear peaks and shoulders in the shape of the release spectra at ~270 and at ~390 °C as highlighted with vertical arrows in Fig. 4. These side peaks can be speculated to be due to loosely bound deuterium on the surface. A similar peak in the H_2 signal can also be observed at this temperature. The D release from the samples 0/1 exposed in ILW-2 and in ILW-3 occurs roughly at the same temperatures. Small Be release (signal intensity typically < 50 cps, not shown in Fig. 4) was also observed starting at ~130 °C. Be signal will not give the full amount of Be in the sample as it is well below the melting temperature. It is only indicative of Be being present on the sample. No Be signal was observed when the same sample was annealed for the second time indicating that no reabsorption of Be occurred. In addition,
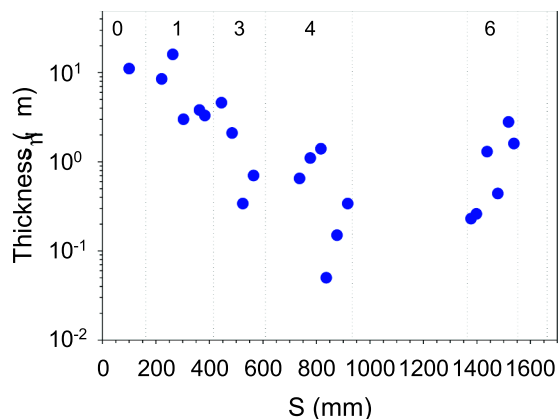
Table 1
Location and D amount of the analysed TDS samples. S-coordinate is the distance around the divertor surface in millimetres. Origin of the S-coordinate is at the left edge of Tile 0.

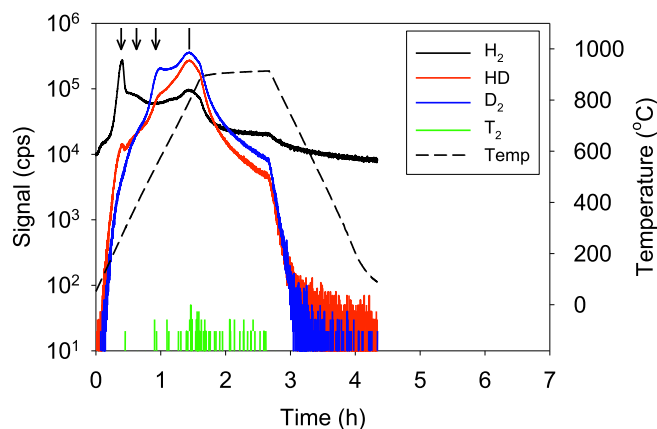| Sample	S-coordinate (mm)	D_2 (10^{15} cm^{-2})	Thickness (μm)
0/5	60	1380	
0/3	100	5080	11.1
0/1	140	3160	
1/10	216	5560	8.5
1/9	243	5350	16.0
1/6	303	2820	3.0
1/3	363	4060	3.8
1/1	403	3690	
3/8	443	4910	4.6
3/6	483	4380	2.1
3/5	503	2480	
3/3	543	2720	0.7
3/1	583	2060	
4/9	754	1150	0.65
4/8	774	3470	1.1
4/5	834	82.5	0.05
4/4	854	205	
4/3	874	569	0.15
6/1	1376	251	0.23
6/4	1436	67.4	1.3
6/6	1476	254	0.44
6/8	1516	1620	2.8
6/9	1536	98	1.6

Fig. 4. TDS spectra and annealing temperature as a function of time for ILW-3 sample 0/1.

the Be release is so small that it does not have effect on interpretation of D release. The W divertor of JET is not actively heated like the Be limiters which are 200 °C. The starting temperature of the different divertor plasma-facing components prior to plasma exposure on the start of an experimental day varies between 90 °C at the apron region and 60 °C at the strike line area [10]. This base temperature rises over a day substantially by interplay of heating during plasma impact and radiative cooling after the plasma pulse, but the start temperature will not be above 120 °C at the apron region prior to a plasma pulse. Therefore, plasma exposition at low surface temperature at low trapping sites can take place.

Fig. 5 shows the TDS results for samples from the top horizontal part of Tile 1 (sample 1/10) exposed either in the ILW-2 or in the ILW-3. The spectra are also fairly broad as was observed with ILW-3 sample 0/1 (Fig. 4). The sharp decrease of the signals at the end is due to emptying of the high energy traps before the hold temperature 910 °C is reached. There is a marked difference between the spectra for the ILW-2 and ILW-3 samples 1/10. The D release for the ILW-2 sample 1/10 occurs at lower temperatures than for the corresponding ILW-3 sample. In Ref. [11] it was observed that the D release occurs at lower temperatures for
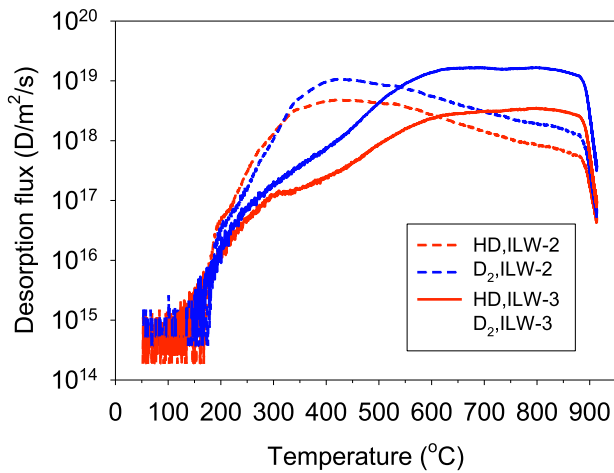

Fig. 3. Thickness of co-deposited layers on top of W/Mo coatings.

Fig. 5. TDS spectra for sample 1/10. Spectra are shown both for the ILW-2 (dashed lines) and ILW-3 samples (solid lines).
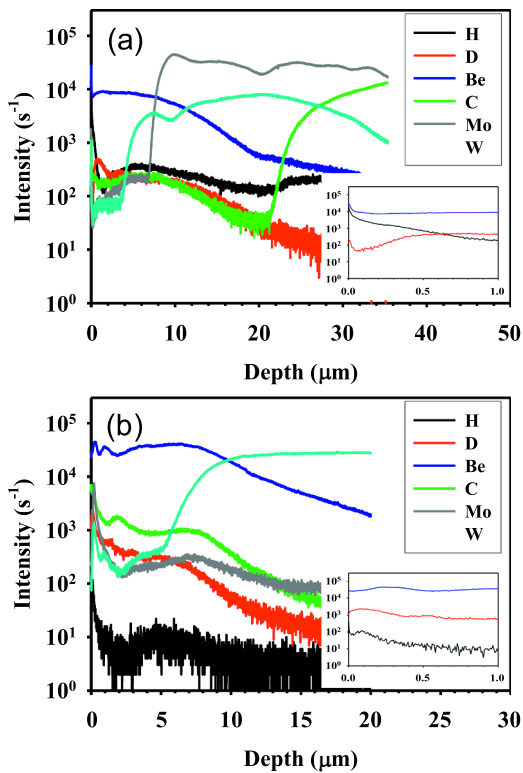

Fig. 6. SIMS depth profiles for Tile 1 apron for ILW-2 (a) and for ILW-3 (b). The insets are expansion of first micron for H, D, Be.

the ILW-2 sample 1/10 than for the ILW-2 sample 0/1. In Refs. [11,12] it was pointed out that the D release occurring at lower temperatures for the sample 1/10 (ILW-2) is related to the thinner co-deposit on the sample and that it has been observed earlier that the thickness of the co-deposit has a significant effect on the D release. However, the co-deposited layer on sample 1/10 (ILW-3) has a thickness of $\sim 8\,\mu m$ as determined by SIMS which is similar to that for sample 0/1 (ILW-3), and the ILW-2 and ILW-3 samples 1/10 also have similar layer thicknesses, so the different release temperatures are not due to differences in the thickness of the deposits. The D amount on the ILW-3 sample 1/10 is somewhat higher than on the ILW-2 sample, $5.7 \times 10^{18}\,cm^{-2}$ (ILW-3) vs. $3.4 \times 10^{18}\,cm^{-2}$ (ILW-2). Be, C and O amounts on both samples are comparable so the impurity amounts do not explain the different release temperatures. There is one main difference between

the ILW-2 and ILW-3 campaigns, the ILW-2 was finished with a two week H plasma campaign. The effect of the H operations can be observed as an H surface peak in SIMS depth profiles (see Fig. 6a). The analysed ILW-2 and ILW-3 samples from the apron of Tile 1 in Fig. 6 have different kinds of W coatings. The ILW-2 sample had a marker coating with a layer structure of CFC (bulk)/Mo $(3\,\mu m)$/W $(12\,\mu m)$/Mo $(4\,\mu m)$/W $(4\,\mu m)$ whereas the ILW-3 sample had a standard 20–25 μm thick W coating. Smearing of Mo and W signals in Fig. 6a is most likely due to roughness of the sample. The inset in Fig. 6a shows a surface peak for H and depletion of D for the ILW-2 sample 1/10, whereas for the ILW3 sample in Fig. 6b D has a near-surface peak and the H amount is clearly smaller than in Fig. 6a. The SIMS results for the H and D amounts in the ILW-2 and ILW-3 samples 1/10 agree qualitatively with the TDS results in Fig. 5. The SIMS results could also indicate that during the two week H operations in ILW-2 the low energy traps near the surface could be filled with H which is then released at lower temperatures and that D is released at higher temperatures. The TDS results do not, however, support this. Therefore it seems that the H campaign at the end of ILW-2 did not have any effect on the release temperatures.

TDS spectra for the sample 1/9 from the upper vertical region of Tile 1 exposed either during ILW-2 or ILW-3 are fairly broad with three D release maxima but as in Fig. 5 for ILW-2 and ILW-3 samples 1/10, the HD and D_2 release occur clearly at higher temperatures for the ILW-3 sample than for the ILW-2 one. This indicates that the low energy traps in the ILW-3 sample have been emptied during the plasma operations and that D is either in the energetically deep traps or located deeper in the sample. The HD and D_2 release start roughly at the same temperature, though. SIMS depth profiling shows that the D concentration is rather uniform in the co-deposited layer. According to the SIMS depth profiling the thicknesses of the co-deposited layers are $\sim 12\,\mu m$ (ILW-2) and $\sim 15\,\mu m$ (ILW-3). The difference in the layer thicknesses is so small that most likely it does not explain the difference in the release temperatures. According to TDS the D amount in the ILW-2 sample 1/9 is nearly double that in the corresponding ILW-3 sample, $1.1 \times 10^{19}\,cm^{-2}$ (ILW-2) vs. $5.4 \times 10^{18}\,cm^{-2}$ (ILW-3). Both SIMS and IBA indicate that the Be amount is slightly higher in the ILW-3 sample than in the ILW-2 sample whereas the C amount is somewhat smaller. As in the case of samples 1/10 the differences in the impurity amounts do not explain the differences in the release temperatures.

The TDS spectra for the ILW-3 sample 1/3 from the lower vertical region of Tile 1 has similar features to the other samples from Tile 1. The TDS spectra for the ILW-3 sample show the HD and D_2 release occur at higher temperatures than for the ILW-2 sample. The first trap at $\sim 400\,°C$ for the ILW-2 samples from Tile 1 seems to be more or less empty in the ILW-3 samples whereas the concentration of the traps at ~ 620 and at $\sim 800\,°C$ is clearly higher in the ILW-3 samples than in the ILW-2 samples (as for 1/10 in Fig. 5). The concentration of the high temperature traps (at ~ 620 and at $\sim 800\,°C$) vary in the ILW-3 samples from Tile 1. In the ILW-3 sample 1/10 (Fig. 5) the traps have similar concentration whereas in the ILW-3 sample 1/9 the trap at $\sim 800\,°C$ has higher concentration than the trap at $\sim 620\,°C$. In the ILW-3 sample 1/3 the trap at $\sim 620\,°C$ has higher concentration than the trap at $\sim 800\,°C$.

During ILW-3 the ISP was on Tile 3 either at $S = 505\,mm$ or at $S = 557\,mm$ (see Fig. 2). According to the SIMS depth profiling, deposits at the top part of Tile 3 with a thickness of $\sim 5\,\mu m$ are observed on the surface overlaying the eroded W/Mo layers. The thickness of the Be co-deposit decreases to $\sim 1\,\mu m$ at the lower part of the tile. The TDS spectra for HD and D_2 molecules from the top (sample 3/8) of Tile 3 are shown in Fig. 7 both for the ILW-1 + ILW-2 and the ILW-3 samples. The spectra for the samples 3/8 exposed in different periods are rather similar in shape and there is slightly more D in the ILW-1 + ILW-2 sample. The ILW-1 + ILW-2 sample has slightly higher temperature for maximum D_2 release ($\sim 520\,°C$ for the ILW-3, $\sim 590\,°C$ for the ILW-1 + ILW-2 sample). In the case of other samples from different poloidal locations on Tile 3, the temperatures for the maximum D release are rather
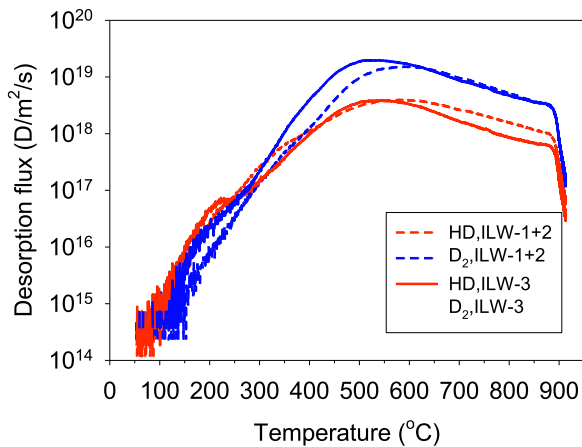
Fig. 7. TDS spectra for sample 3/8. Spectra are shown both for ILW-1 + ILW-2 and ILW-3 samples.

Fig. 8. TDS spectra for sample 4/8. Spectra are shown both for ILW-2 and ILW-3 samples.

similar for the ILW-2 and the ILW-3 samples. The shape of the spectra for the ILW-1 + ILW-2 and the ILW-3 samples are rather similar. Release of Be was also observed with the TDS from the sample near the top region of the tile whereas near the bottom hardly any Be was released. In Ref. [11] it was observed that D is released at higher temperatures from Tile 3 than from Tile 1 whereas in the case of the ILW-3 samples from Tiles 1 and 3, maximum D release occurs roughly at same temperatures. The D release from the ILW-3 samples from Tile 3 is at higher temperature than for the ILW-1 + ILW-2 samples.

3.2. Divertor base

During ILW-2 and ILW-3 there were more low delta discharges than during ILW-1, i.e. strike points on Tiles 4 and 6. The ISP on Tile 4 was mainly on the sloping part which changed the migration pattern allowing more transport towards Tile 4. There is some deposition on Tile 4 and the measured Be amount is up to 1.5 times higher at the deposition region ($S = 770$ mm) after ILW-3 than after ILW-2. After ILW-2 it was observed that the Be and D deposition extends also to the plasma shadowed region at the inner corner of the divertor [13]. After ILW-3 the Be and D deposition at the inner corner was not observed. TDS spectra for the ILW-2 and the ILW-3 sample 4/3 from the top horizontal part are fairly broad with two D release maxima but the ILW-3 sample has slightly higher release temperature for D (ILW-2 ~420 °C, ILW-3 ~550 °C). The ILW-3 sample has somewhat less D than the ILW-2 sample, 1.5×10^{18} cm^{-2} (ILW-2), 8.7×10^{17} cm^{-2} (ILW-3). The TDS spectra for the ILW-3 sample 4/8 located at the bottom of the sloping part of the tile has similar features to the ILW-3 sample 4/3 (see Fig. 8). The D release starts at a temperature of ~ 190 °C. The HD and D$_2$ spectra for the ILW-3 sample are broad and they have a smaller peak at ~280 °C similarly to the ILW-2 sample. There is no systematic correlation in the impurity amounts between the spectra for the samples 4/8. Fig. 8 shows that the D content is slightly smaller for the ILW-3 sample. In addition, the C amount is smaller for the ILW-3 sample than for the ILW-2 sample (1.8×10^{18} cm^{-2} vs. 8.6×10^{18} cm^{-2}) but the Be content is higher for the ILW-3 sample (7.5×10^{18} cm^{-2} vs. 5.3×10^{18} cm^{-2}). The ISP time was slightly higher at $S = 800$ mm for the ILW-3 than for the ILW-2. The transport mechanism towards the relatively cooler remote surfaces in the shadowed region of Tile 4 during these discharges with the ISP at $S = 800$ mm is similar for both campaigns and as a consequence line of sight transport from the ISP location to relatively cooler remote surfaces but the impurity fluxes are different as observed in the IBA analyses.

During ILW-3 the OSP was mainly on the sloping part of Tile 6 at $S = 1486$ mm as it was for ILW-2. Analogous to Tile 4, a deposition band outboard of the OSP location with a thickness ~2–4 µm was
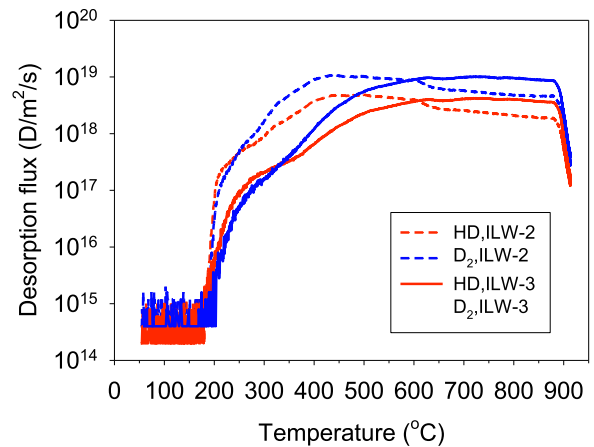
observed at $S = 1511$ mm. The thickness of the co-deposit on Tile 6 exposed during ILW-3 is, however, thinner than on Tile 6 exposed for two campaigns (ILW-1 + ILW-2). In the shadowed region of this Tile 6, the SIMS depth profiling showed the thickness of the deposit to be over 10 µm [6]. However, for most of the samples from the ILW-3 Tile 6 the thickness of the deposit is less than 1 µm.

The TDS spectra for the sample 6/4 exposed for two campaigns (ILW-1 + ILW-2) have release maxima at ~ 500 °C and there is a smaller component at ~ 610 °C. The spectra for the ILW-3 sample 6/4 are broader and they have two release maxima at ~ 430 and at ~ 620 °C. The maximum at ~ 620 °C is more intense in the ILW-3 sample than in the ILW-1 + ILW-2 sample indicating that the concentration of deep traps is higher in the ILW-3 sample. The TDS spectra for the ILW-1 + ILW-2 and ILW-3 samples 6/6 from the sloping part have different shapes. The HD and D$_2$ signals from the ILW-1 + ILW-2 sample 6/6 which was located near the OSP have three release maxima at ~290, ~570 and ~870 °C, the maximum at ~570 °C being the strongest. The ILW-3 sample has only two release maxima at ~430 and ~ 870 °C and there is a dip at ~620 °C. The D amount on the ILW-3 sample seems to be higher than on the ILW-1 + ILW-2 sample even though both samples were located near the OSP. The D amount near the OSP is smaller than elsewhere on Tile 6 for the ILW-1 + ILW-2 samples but not in the case of the ILW-3 samples. The TDS spectra for the sample 6/9 from the shadowed region are shown in Fig. 9. Both the spectra for ILW-1 + ILW-2 and ILW-3 samples are broad and the maximum D release occurs at temperatures > 700 °C. The spectra for D$_2$ are rather similar but the ILW-1 + ILW-2 spectra are somewhat broader. In addition, the
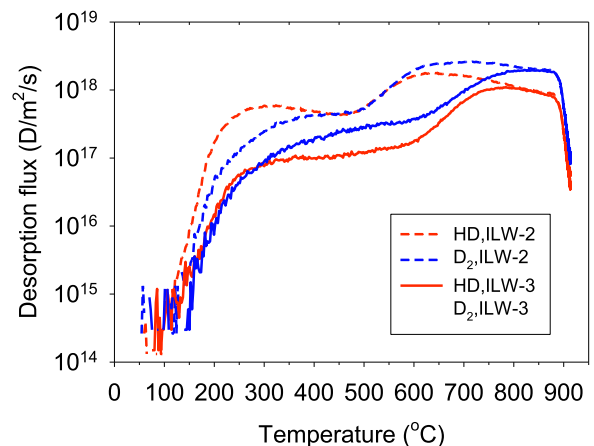

Fig. 9. TDS spectra for sample 6/9. Spectra are shown both for ILW-2 and ILW-3 samples.
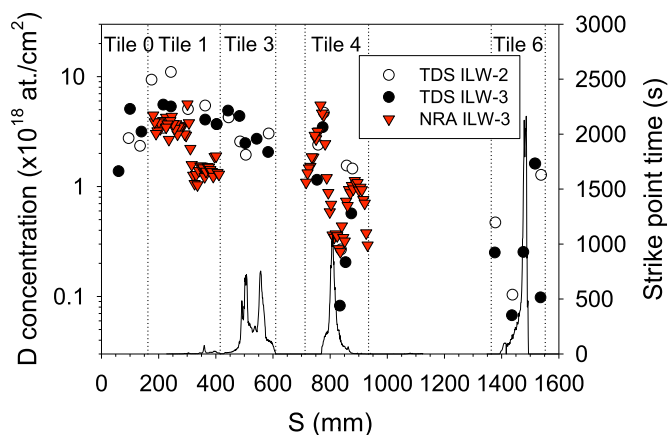
Fig. 10. D amount on Tiles 0, 1, 3, 4 and 6 measured with TDS and NRA. TDS ILW-2 corresponds to TDS analyses made from ILW-2 tiles. NRA results are for ILW-3. The strike point distribution for ILW-3 is also shown.

spectra for the ILW-3 sample have been shifted to higher temperatures. In Refs. [11,14] it was observed that in general the TDS spectra for the ILW-1 samples have release maxima at lower temperatures than the corresponding spectra for the ILW-2 samples. This was partly related to lower absorbed energies used during the ILW-1 campaign, as higher tile temperatures in the plasma wetted areas lead to D out-diffusion especially from the low energy traps. Higher release temperatures for the ILW-3 samples than for the corresponding ILW-2 samples could be due to higher absorbed energies [15].

The poloidal distribution of D on divertor Tiles 0, 1, 3, 4 and 6 together with the strike point distributions is shown in Fig. 10. Comparison is made between TDS and NRA data. The NRA data is available only for Tiles 1 and 4 at the moment. The highest D amounts are on Tile 0 and on the apron of Tile 1. There seems to be somewhat more D on the ILW-3 Tile 0 than on the ILW-2 tile but somewhat less on ILW-3 Tile 1 than on the ILW-2 tile. Agreement between TDS and NRA is good on the apron of Tile 1 and on the upper vertical region of Tile 1 whereas on the lower vertical region of Tile 1 the NRA results are clearly smaller than the TDS results. The co-deposit on the upper vertical region of Tile 1 is thicker than at the lower vertical region and the D profiles extend deeper in the upper vertical region where the agreement between TDS and NRA is good. This means that the discrepancy at the lower vertical region is not directly related to smaller analysis depth of NRA. In the case of Tile 3 there is more D on the upper vertical region than on the lower region. Both the ILW-2 and ILW-3 tiles seem to have similar D amounts but the ILW-2 tile was exposed for two campaigns, i.e. for the ILW-1 + ILW-2, so the deposition rate for D was higher for the ILW-3 tile.

The TDS results indicate that the D amounts on Tile 4 are somewhat smaller for the ILW-3 samples than for the ILW-2 samples. The NRA results follow similar pattern for the D deposition as a function of the S coordinate showing a dip inboard of the ISP location at $S = 806$ mm. The ISP time was comparable at $S = 800$ mm for the ILW-2 and for the ILW-3. The impurity fluxes onto Tile 4 are somewhat different for the ILW-2 and the ILW-3 as observed in the IBA analyses. The Be flux onto Tile 4 was higher for the ILW-3 than for the ILW-2. In the case of the C flux onto Tile 4 the C amounts in the shadowed region of Tile 4 are comparable but there is more C deposition on the sloping part of Tile 4 for ILW-2 than for ILW-3. On the top horizontal part of Tile 4 there is somewhat less deposition for ILW-2 than for ILW-3.

ILW-2 Tile 6 was exposed for two campaigns (ILW-1 + ILW-2) explaining higher D amounts when compared with ILW-3. Near the main OSP location there is a minimum in the D amount indicating D release near the OSP due to high absorbed energies. The D amount increases towards the shadowed region of Tile 6 for the ILW-2 samples but not for the ILW-3 samples as there is more than an order of magnitude

difference between the ILW-2 and the ILW-3 samples. The D retention at the divertor inner and outer corner regions is not symmetric as there is more D retention poloidally at the inner than at the outer divertor corner.

There was an overall increase in the absorbed energies at the divertor tiles in ILW-3 when compared with ILW-2 [15,16] which may have increased the surface temperatures of the divertor tiles. The surface temperatures of the divertor tiles are measured at JET using IR cameras but there is no systematic temperature distribution as a function of S-coordinate for the whole experimental campaign because of various kinds of plasma configurations applied. In addition, the emissivities are not known accurately e.g. for the upper inner divertor region with thick co-deposited layers which complicates determination of the surface temperatures. Wide angle IR camera at JET gives rather uniform temperature distribution with temperature values of ~200 °C for H-mode discharges across the divertor. There are, however, indications that the surface temperature at the upper inner divertor region may increase to high temperatures during discharges but peak temperatures are not known accurately.

4. Conclusions

TDS has been used to analyse samples from the W-coated CFC divertor tiles exposed during the ILW-3 campaign in 2015–2016. As was during the ILW-1 and ILW-2 campaigns, in ILW-3 the fuel retention was 10–20 times smaller than measured during the JET all-carbon wall campaign 2007–2009. In addition, the highest amount of deuterium was found on the regions with the thickest co-deposited layers, i.e. on Tile 0 and on the top horizontal part and at the top of plasma-facing surface of Tile 1. The D amounts obtained with TDS were compared with the NRA measurements and agreement between TDS and NRA was good in the case of Tile 0, the apron of Tile 1 and the top vertical region of Tile 1 whereas on the lower vertical region of Tile 1 TDS results are clearly higher than the NRA results. The D retention at the divertor inner and outer corner regions is not symmetric as there is more D retention poloidally at the inner than at the outer divertor corner. In most cases the TDS spectra for the ILW-3 samples are different from the corresponding ILW-2 spectra because the HD and D_2 release occurs at higher temperatures indicating that the low energy traps have been emptied. The impurity amounts and the thickness of the co-deposited layers are comparable so these do not explain the differences in the release temperatures. In addition, the two week H operation at the end of ILW-2 is not perhaps the reason for lower release temperatures of the ILW-2 samples. Higher release temperatures for the ILW-3 samples than for the corresponding ILW-2 samples could be due to higher absorbed energies.

References

[1] K. Heinola, J.L. A.Widdowson, E. Alves, A. Baron-Wiechec, N. Barradas, S. Brezinsek, N. Catarino, J.P. Coad, S. Koivuranta, S. Krat, G.F. Matthews, M. Mayer, P. Petersson, Phys. Scr. T167 (2016) 014075.
[2] S. Brezinsek, T. Loarer, V. Philipps, et al. Nucl. Fusion 53 (2013) 083023.
[3] A. Widdowson, E. Alves, C.F. Ayres, A. Baron-Wiechec, S. Brezinsek, N. Catarino, J.P. Coad, K. Heinola, J. Likonen, G.F. Matthews, M. Mayer, M. Rubel, Phys. Scr. T159 (2014) 014010.
[4] J.P. Coad, E. Alves, N.P. Barradas, A. Baron-Wiechec, N. Catarino, K. Heinola,

J. Likonen, M. Mayer, G.F. Matthews, P. Petersson, A. Widdowson, Phys. Scr. T159 (2014) 014012.

[5] I. Nunes, S. Brezinsek, J. Buchanan, et al. 26th IAEA Fusion Energy Conference, paper paper PDP-2, Kyoto, Japan, October, 2016, pp. 17–22.

[6] A. Lahtinen, J. Likonen, S. Koivuranta, A. Hakola, K. Heinola, C.F. Ayres, J.P. Coad, A. Widdowson, J. Räisänen, Nucl. Mater. Energy 12 (2017) 655.

[7] A. Baron-Wiechec, K. Heinola, J. Likonen, E. Alves, N. Catarino, J.P. Coad, V. Corregidor, I. Jepu, G.F. Matthews, A. Widdowson, Fusion Eng. Des. 133 (2018) 135.

[8] T. Ahlgren, K. Heinola, K. Vortler, J. Keinonen, J. Nucl. Mater. 427 (2012) 152.

[9] N. Catarino, N.P. Barradas, V. Corregidor, A. Widdowson, A. Baron-Wiechec, J.P. Coad, K. Heinola, M. Rubel, E. Alves, Nucl. Mater. Energy 12 (2017) 559.

[10] S. Brezinsek, S. Wiesen, D. Harting, C. Guillemaut, A.J. Webster, K. Heinola, A.G. Meigs, M. Rack, Y. Gao, G. Sergienko, Phys. Scr. T167 (2016) 014076.

[11] J. Likonen, K. Heinola, A. De Backer, A. Baron-Wiechec, I. Jepu, C.F. Ayres,

J.P. Coad, S. Koivuranta, S. Krat, G.F. Matthews, M. Mayer, A. Widdowson, Nucl. Mater. Energy 19 (2019) 166.

[12] K. Heinola, J. Likonen, T. Ahlgren, S. Brezinsek, G. De Temmerman, I. Jepu, G.F. Matthews, R.A. Pitts, A. Widdowson, Nucl. Fusion 57 (2017) 0860024.

[13] A. Widdowson, E. Alves, A. Baron-Wiechec, N.P. Barradas, N. Catarino, J.P. Coad, V. Corregidor, A. Garcia-Carrasco, K. Heinola, S. Koivuranta, S. Krat, A. Lahtinen, J. Likonen, M. Mayer, P. Petersson, M. Rubel, S. Van Boxel, Nucl. Mater. Energy 12 (2017) 499.

[14] J. Likonen, K. Heinola, A. De Backer, S. Koivuranta, A. Hakola, C.F. Ayres, A. Baron-Wiechec, J.P. Coad, G.F. Matthews, M. Mayer, A. Widdowson, Phys. Scr. T167 (2016) 014074.

[15] K. Heinola, Private communication.

[16] K. Heinola, A. Widdowson, J. Likonen, T. Ahlgren, E. Alves, C.F. Ayres, A. Baron-Wiechec, N. Barradas, S. Brezinsek, N. Catarino, P. Coad, C. Guillemaut, I. Jepu, S. Krat, A. Lahtinen, G.F. Matthews, M. Mayer, Phys. Scr. T170 (2017) 014063.